**Proceedings of 9th International Symposium on Fluid-Structure Interactions, Flow-Sound Interactions, Flow-Induced Vibration & Noise**
**July 8-11, 2018, Toronto, Ontario, Canada**

**FIV2018-031**

# A NUMERICAL STUDY OF VIV SUPPRESSION USING A ROTATIVE NON-LINEAR VIBRATION ABSORBER (NVA) AND A WAKE-OSCILLATOR MODEL

**Tatiana Ueno**
ueno.tatiana@gmail.com

**Beatriz S. Sato**
beatriz.sayuri.sato@usp.br

**Guiherme R. Franzini**
gfranzini@usp.br

Offshore Mechanics Laboratory (LMO), Escola Politécnica, University of São Paulo, São Paulo, SP, Brazil

## ABSTRACT

*Vortex-induced vibrations (VIV) suppression is an important aspect on riser dynamics. In this paper, a type of passive suppressor named NVA (non-linear vibration absorber) is numerically studied aiming at controlling the VIV of a rigid and elastically supported cylinder. The cylinder is constrained to oscillate only in the cross-wise direction and the hydrodynamic loads are modeled using a wake-oscillator approach. The response of the system composed of the cylinder and the suppressor is presented as a function of three parameters that define the NVA (namely, its mass,* radius *and dashpot constant) for different reduced velocities. Two quantitative criteria are defined and examples of cylinder and NVA responses are presented. Among other findings, the paper shows that the mass of the suppressor has more influence on the VIV suppression than the other parameters.*

## NOMENCLATURE

$\xi_\theta$, $\xi_y$ NVA and cylinder damping ratio, respectively
$\omega_y$ Natural frequency of the cylinder
$\hat{m}$ Ratio between the mass of the NVA and the mass of the cylinder
$\hat{r}$ Ratio between the *radius* of the NVA and the diameter of the cylinder
$S$, $S^*$ NVA effectiveness criteria based on the areas below response curve and on the maximum response amplitude, respectively
$y$, $\theta$ Dimensionless cylinder and NVA responses, respectively
$q$ Wake-oscillator variable
$A$, $\varepsilon$ Empirical parameters of the wake-oscillator models
$C_L^0$, $C_{D,V}$ Amplitude of the lift coefficient and mean drag coefficient observed for a fixed cylinder, respectively
$\hat{A}$ Cylinder characteristic oscillation amplitude
$V_R$ Reduced velocity

## INTRODUCTION

The vortex-induced vibration (VIV) phenomenon is a relevant topic in ocean engineering, since it may decrease the lifespan of risers due to structural fatigue. Commonly observed on slender structures, VIV is characterized as a self-excited and self-limited phenomenon, presenting maximum oscillation amplitudes close to one diameter. Further aspects of the phenomenon can be found in the textbooks [1] and [2] and in a series of papers such as [3] and [4].

The VIV analyses are usually carried out follow-

ing three approaches: laboratory experiments, high-hierarquical numerical investigations (Computational Fluid Dynamics - CFD) simulations and reduced-order modeling using phenomenological models. The latter, focus of this paper, is also known as wake-oscillator approach and employs non-linear equations aiming at representing the wake dynamics. The non-linear equation (for example, the van der Pol equation) is coupled to the structural oscillator by means of some empirically determined parameters. The wake-oscillator approach has received numerous efforts in the last decades since it requires low computational cost (when compared to CFD) and it can be used for theoretical studies. Examples of VIV studies using wake-oscillators can be found in [5] and [6].

Among different aspects of the phenomenon, VIV suppression has motivated many efforts. Strakes and splitter-plates are examples of suppressors that are in direct contact with the external flow. Conversely, there is another type of devices named non-linear vibration absorber (NVA). The NVA herein investigated consists of a mass internally assembled to the main structure by means of a dashpot and is characterized by an intrinsic non-linear dynamic (i.e, non-linearizable natural frequency). Such a kind of NVA is also named as non-linear energy sinks (NES).

When this strong non-linearity is added, broadband and irreversible energy transfer from the main structure (in this paper, the main cylinder) to the NVA occurs. At the NVA's dashpot, part of its energy is dissipated. Such an energy transfer is known as Target Energy Transfer (TET). Further theoretical discussions regarding TET can be found in a series of recent contributions (for example, [7]). The references [8] and [9] are examples of works on passive suppression of VIV using NVAs, despite employing different approaches from that proposed in this paper.

This paper aims at presenting examples of analyses of the system composed of the cylinder and the rotative NVA subjected to VIV. Contrary to previous papers in which the hydrodynamic load is computed from CFD and the results are presented as functions of the Reynolds number (see, for example, [8] and [10]), herein we evaluate the hydrodynamic load using the wake-oscillator model presented in [6]. For different set of NVA parameters, oscillation amplitudes are obtained for a series of values of reduced velocity covering the lock-in range. At least to the authors' knowledge, both the numerical study of VIV suppression using a rotative NVA by means of the wake-oscillator approach and the systematic experimental investigations on this theme are not found in the literature.

## MATHEMATICAL MODEL

This paper focuses on the problem of a rigid cylinder, subject to VIV and mounted on an elastic support with linear stiffness $k$ and damping $c$. This cylinder has mass $M$ , diameter $D$, length $L$ and is immersed in a stationary and uniform flow of free stream velocity $U_\infty$. The fluid has density $\rho$. The rotative NVA consists of a massless rigid bar of length $r$ with a tip mass $m$. The rigid bar is linked to the cylinder by using a viscoelastic device of stiffness $k_\theta$ and damping $c_\theta$. A schematic representation of the problem is presented in Fig.1.

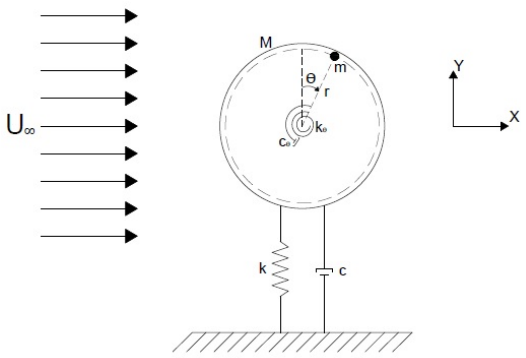


**FIGURE 1**: MODEL REPRESENTATION.

The equations of motion are derived using the Euler-Lagrange's equation. The variables $Y$, $\theta$ and $q$ are the generalized coordinates referring to the cross-wise displacement of the cylinder, the rotation of NVA and the variable of wake-oscillator model respectively. For the sake of conciseness of the paper, the expressions for both the kinetic and the potential energy are not presented.

The virtual work of the non-conservative forces is defined as:

$$\delta W^{nc} = \left( F_H - c\frac{dY}{dt} - m_a\frac{d^2Y}{dt^2} \right) \delta Y - \left( c_\theta \frac{d\theta}{dt} \right) \delta\theta \quad (1)$$

where $t$ is dimensional time. The hydrodynamic load is decomposed into a term proportional to the acceleration of the cylinder ($m_a$ is the added mass) and a term

associated with VIV ($F_H$). As already mentioned, $F_H$ is modeled using the wake-oscillator model presented in [6], who decompose the cross-wise vortex force coefficient $C_{V,Y}$ into drag ($C_{V,D}$) and lift ($C_{V,L}$) components. Based on the Euler-Lagrange's equation and the mentioned wake-oscillator model, the dynamics of the hydro-elastic system composed by the cylinder, the NVA and the fluid are governed by the following dimensional equations:

$$(M+m+m_a)\frac{d^2Y}{dt^2} - mr\sin\theta\frac{d^2\theta}{dt^2} + c\frac{dY}{dt} + kY - \\ -mr\cos\theta\left(\frac{d\theta}{dt}\right)^2 = F_H = \frac{1}{2}\rho U_\infty^2 DLC_{V,Y} \quad (2)$$

$$mr^2\frac{d^2\theta}{dt^2} - mr\sin\theta\frac{d^2Y}{dt^2} + c_\theta\frac{d\theta}{dt} + k_\theta\theta = 0 \quad (3)$$

$$\frac{d^2q}{dt^2} + \varepsilon\omega_s(q^2-1)\frac{dq}{dt} + \omega_s^2 q = \frac{A}{D}\frac{d^2Y}{dt^2} \quad (4)$$

In Eq. 4, $\omega_s$ is the vortex-shedding frequency and $A$ and $\varepsilon$ are parameters from the wake-oscillator model that must be calibrated from pure VIV experiments. In this paper, $A$ and $\varepsilon$ follow the suggestions made in [6].

A series of quantities can be defined as follows:

$$y = \frac{Y}{D}; \quad \hat{r} = \frac{r}{D}; \quad \hat{m} = \frac{m}{M}; \quad m^* = \frac{4(M+m)}{\rho\pi D^2 L};$$
$$\omega_y = \sqrt{\frac{k}{(M+m+m_a)}}; \quad \omega_\theta = \sqrt{\frac{k_\theta}{mr^2}}; \quad \Omega = \frac{\omega_\theta}{\omega_y};$$
$$\xi_y = \frac{c}{2(M+m+m_a)\omega_y}; \quad \xi_\theta = \frac{c_\theta}{2mr^2\omega_y}; \quad \tau = \omega_y t;$$
$$St = \frac{\omega_s D}{2\pi U_\infty}; \quad V_R = \frac{U_\infty 2\pi}{\omega_y D}; \quad C_a = \frac{4m_a}{\rho\pi D^2 L} \quad (5)$$

Notice that, in the above quantities, $m^*$ is the mass ratio parameter, $V_R$ is the reduced velocity and $St$ is the Strouhal number. The wake variable $q$ is linearly proportional to lift coefficient in the form $q = \frac{C_{V,L}}{C_L^0}\hat{q}$, in which $C_L^0$ is amplitude of the lift coefficient for a fixed cylinder and $\hat{q} = 2$ is the amplitude of the limit cycle of Eq. 4 when its right-hand side is null.

Hereafter, $(\dot{\ })$ indicates the derivative with respect to the dimensionless time $\tau$. By substituting the quantities presented in Eq. 5 into Eqs. 2 to 4, we obtain Eqs. 6 to 8, corresponding to the dimensionless equations of motion of the hydro-elastic system:

$$\ddot{y} - \left(\frac{\hat{m}}{1+\hat{m}}\right)\left(\frac{m^*}{1+m^*}\right)\hat{r}\left(\sin\theta\ddot{\theta} + \cos\theta\left(\dot{\theta}\right)^2\right) + \\ + 2\xi_y\dot{y} + y = \\ = \frac{V_R^2}{2\pi^3(C_a+m^*)}\sqrt{1+\left(\frac{2\pi}{V_R}\dot{y}\right)^2}\left(\frac{C_L^0}{\hat{q}}q - \frac{2\pi}{V_R}C_{V,D}\dot{y}\right) \quad (6)$$

$$\ddot{\theta} - \frac{1}{\hat{r}}\sin\theta\ddot{y} + 2\xi_\theta\dot{\theta} + \Omega^2\theta = 0 \quad (7)$$

$$\ddot{q} + \varepsilon StV_R(q^2-1)\dot{q} + (StV_R)^2 q = A\ddot{y} \quad (8)$$

$C_{V,D}$ being the mean drag coefficient observed for a fixed cylinder.

## ANALYSIS METHODOLOGY

Eqs. 6 to 8 are numerically integrated using MATLAB® ode45 function (Runge-Kutta method). The time-step is $\Delta\tau = 0.01$ and the maximum dimensionless time is $\tau_{max} = 800$. The adopted initial conditions are $y(0) = 0$, $\dot{y}(0) = 0$, $q(0) = 0.10$, $\dot{q}(0) = 0$, $\theta(0) = \pi/6$ and $\dot{\theta}(0) = 0$.

The effect of the rotative NVA on the cylinder response is studied for $2 < V_R < 14$, covering the lock-in range of reduced velocities. Characteristic oscillation amplitudes $\hat{A}$ are determined from the standard deviation of the corresponding steady-state time history using $\hat{A} = \sqrt{2}std(y)$. In this paper, steady-state responses are considered for $\tau > \tau_{max}/2$.

As mentioned, we use both the wake-oscillator model and the empirical parameters $A$ and $\varepsilon$ presented in [6]. For the upper branch, the authors uses $A = 4$ and $\varepsilon = 0.05$ and for the lower branch, they suggest $A = 12$ and $\varepsilon = 0.7$. The same reference suggests $C_L^0 = 0.3842$, $St = 0.1932$ and $C_{D,v} = 1.1856$. The transition from the upper branch to the lower branch is herein defined as occurring at $V_R = 6.5$ and added mass coefficient $C_a$ is taken as unitary.

The parameters of the cylinder are adopted according to the experimental investigation presented in [11], namely $m^* = 2.6$ and $\xi_y = 0.0008$. Even though the mathematical model considers the presence of the torsional spring of constant $k_\theta$, we investigate the case in which the NVA is characterized by an essentially non-linear dynamics. Hence, we assume $\Omega = 0$.

Aiming at studying the influence of the NVA parameters on the cylinder response, the values of $\hat{m}$, $\hat{r}$ and $\xi_\theta$ are systematically varied. For the sake of organization,

Tab. 1 presents three simulation groups. In each group, two parameters are fixed and the third one varies with respect to a reference case, identified as "Sim-0". The reference case is characterized by $\hat{m} = 0.05$, $\hat{r} = 0.50$ and $\xi_\theta = 0.10$. Another condition also studied is that without NVA, herein named as "Pure VIV".

**TABLE 1**: SIMULATION GROUPS.

| Group 1 $\hat{r} = 0.50$ $\xi_\theta = 0.10$ | | Group 2 $\hat{m} = 0.05$ $\xi_\theta = 0.10$ | | Group 3 $\hat{m} = 0.05$ $\hat{r} = 0.50$ | |
|---|---|---|---|---|---|
| Sim | $\hat{m}$ | Sim | $\hat{r}$ | Sim | $\xi_\theta$ |
| G1-Sim1 | 0.03 | G2-Sim1 | 0.40 | G3-Sim1 | 0.20 |
| G1-Sim2 | 0.07 | G2-Sim2 | 0.30 | G3-Sim2 | 0.15 |
| G1-Sim3 | 0.10 | G2-Sim3 | 0.20 | G3-Sim3 | 0.08 |
| G1-Sim4 | 0.12 | G2-Sim4 | 0.10 | G3-Sim4 | 0.05 |
| G1-Sim5 | 0.15 | | | G3-Sim5 | 0.01 |

Besides the analysis of the characteristic oscillation amplitude as a function of the reduced velocity, we quantify the suppression efficiency. For this, we employ two criteria originally proposed in [12] for the analysis of strakes. The first one is given by Eq. 9 and considers only the ratio between the maximum characteristic oscillation amplitude reached by the cylinder in the cases with the NVA ($\max\{\hat{A}_{NVA}\}$) and without it ($\max\{\hat{A}_{pure}\}$).

The second criterion is given by Eq. 10 and considers the area below the curve $\hat{A} \times V_R$. In this criterion $Ar_{NVA}$ and $Ar_{pure}$ refer, respectively, to the areas obtained with and without the NVA. Notice that the criteria based on $S^*$ considers only the maximum characteristic oscillation amplitude, whereas the use of $S$ refers to the whole range of reduced velocities in which VIV occurs.

$$S^* = 1 - \frac{\max\{\hat{A}_{NVA}\}}{\max\{\hat{A}_{pure}\}} \tag{9}$$

$$S = 1 - \frac{Ar_{NVA}}{Ar_{pure}} \tag{10}$$

## RESULTS AND DISCUSSION

For the sake of correlation with experimental data, Fig. 2 presents the values of $\hat{A}$ obtained from the Pure VIV simulation plotted onto the experimental data presented in [11]. This plot reveals that the wake-oscillator model herein considered leads to cylinder responses whose characteristic oscillation amplitude very well agree with experimental data.

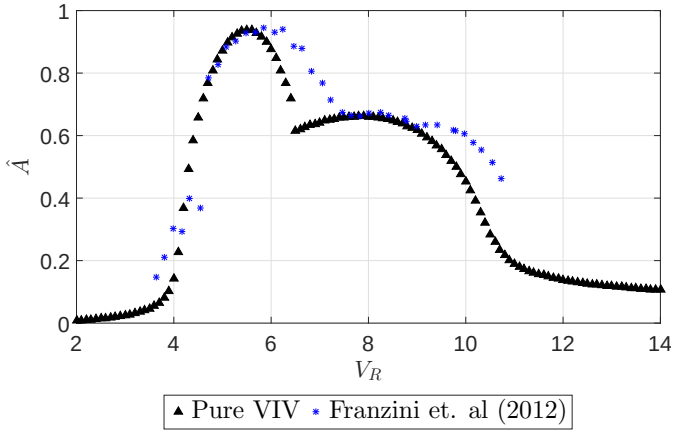


**FIGURE 2**: PURE VIV SIMULATION AND EXPERIMENTAL DATA.

As the mathematical model for pure VIV is validated with experimental data, we focus on the analysis of the system fitted with the NVA. Firstly, we analyze the effects of variation of the parameter $\hat{m}$ (Group 1). Fig. 3 reveals that the NVA has no effect for $V_R < 4.2$. In the lock-in range of reduced velocities, an increase in $\hat{m}$ causes a decrease in the characteristic oscillation amplitudes of the cylinder. Furthermore, the maximum amplitude is observed for a slightly lower reduced velocity in the cases G1-Sim4 and G1-Sim5.

Within the interval $9.0 < V_R < 10.4$, the cases G1-Sim4 and G1-Sim5 lead to larger oscillation amplitudes than the other conditions pertaining to Group 1. Notice, however, that the NVA still suppress VIV. At $V_R \approx 10.5$ the characteristic oscillation amplitude for cases with the NVA are slightly larger than that for pure VIV. Finally, the rotative NVA is not effective and the characteristic oscillation amplitudes match the results for pure VIV for $V_R > 10.7$. It is interesting to point out that significant reduction in $\hat{A}$ is achieved both at the upper branch and at the lower branch if $\hat{m} > 0.10$ (G1-Sim4 and G1-Sim5).

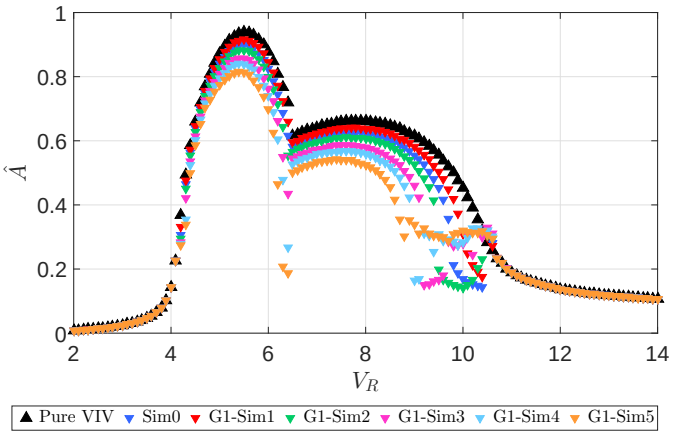


**FIGURE 3**: CHARACTERISTIC OSCILLATION AMPLITUDE CURVE - GROUP 1

Now, we change the focus for the simulations pertaining to Group 2. As can be seen in Fig. 4, the suppression is less sensitive to variation in the *radius* of the NVA than modifications in its mass. Notice also that the peak of the cylinder response occurs at the same reduced velocity $V_R \approx 5.5$ for all simulations. We also point out that the larger the *radius* of the NVA, the smaller is the lock-in region, which is certainly is of importance for VIV suppression.

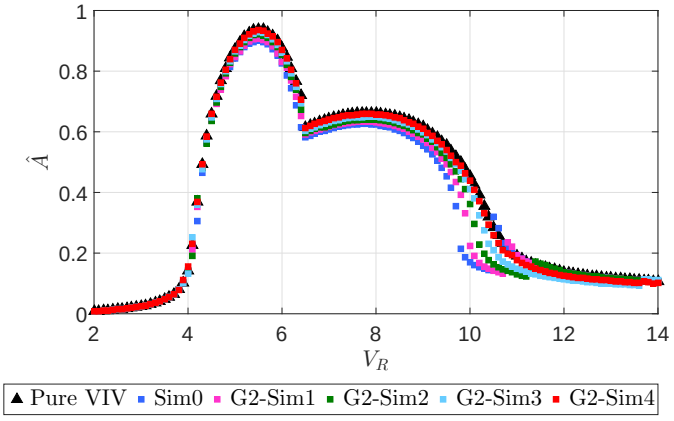


**FIGURE 4**: CHARACTERISTIC OSCILLATION AMPLITUDE CURVE - GROUP 2

The influence of the NVA damping $\xi_\theta$ can be assessed from Fig. 5. As in Group 1 simulations, the onset of the suppression occurs at $V_R \approx 4.1$ and the maximum response is observe at $V_R \approx 5.5$ irrespective of the value $\xi_\theta$. Notice also that the cases G3-Sim1 and G3-Sim2 (corresponding to the higher values of $\xi_\theta$ simulated) exhibit irregular behaviour in the ranges $9.7 < V_R < 10.1$ and $10.0 < V_R < 10.6$, respectively. After this interval, the NVA is no longer effective.

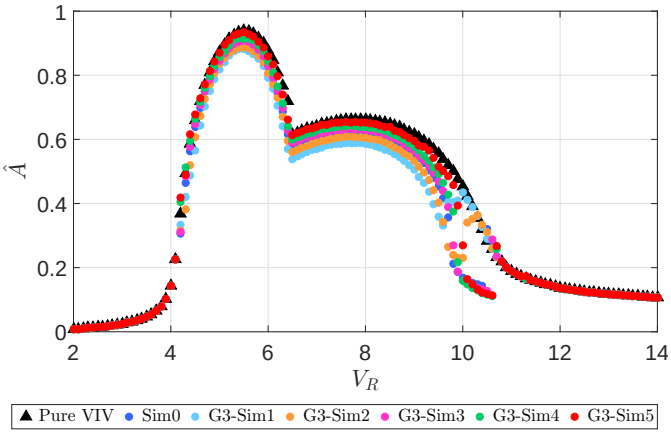


**FIGURE 5**: CHARACTERISTIC OSCILLATION AMPLITUDE CURVE. GROUP 3.

Now, we discuss quantitative aspects of the suppression. For this, consider the values of $S$ and $S^*$ presented in Tab. 2. Notice that, in general, the simulations pertaining to Group 1 have the higher values, being the case G1-Sim5 that with the best set of parameters. The criterion $S$ results are higher than those related to the $S^*$ criterion for all simulations, indicating the suppression does not occur only at the reduced velocity in which the maximum response is reached.

The last discussion of this paper is related to the qualitative aspects of the response. Such an analysis is of great interest and complements the previous ones. For the sake of limitation in the size of the paper, only two time histories are presented, namely the responses of the cylinder with the NVA (Fig. 6(b)) and without it (Fig. 6(a)) at $V_R = 6.4$. The selected response corresponds to the NVA parameters from the simulation G1-Sim5.

The comparison between these time histories allow to highlight two aspects. The first one is the marked reduction in the steady-state oscillations, dropping from $\hat{A} = 0.719$ for pure VIV to $\hat{A} = 0.187$ for the investigated NVA. The second feature is the response of the suppressor, characterized by a practically constant angular velocity. Contrary to the present paper, the cross-wise responses of the controlled structures numerically obtained

**TABLE 2**: NUMERICAL VALUES OF $S$ AND $S^*$.

| Sim | $S^*$ | $S$ | Sim | $S^*$ | $S$ |
|---|---|---|---|---|---|
| Sim-0 | 0.041 | 0.091 | G2-Sim3 | 0.010 | 0.043 |
| G1-Sim1 | 0.024 | 0.051 | G2-Sim4 | 0.003 | 0.016 |
| G1-Sim2 | 0.060 | 0.128 | G3-Sim1 | 0.060 | 0.104 |
| G1-Sim3 | 0.086 | 0.159 | G3-Sim2 | 0.054 | 0.098 |
| G1-Sim4 | 0.105 | 0.180 | G3-Sim3 | 0.033 | 0.084 |
| G1-Sim5 | 0.130 | 0.215 | G3-Sim4 | 0.024 | 0.069 |
| G2-Sim1 | 0.033 | 0.073 | G3-Sim5 | 0.004 | 0.041 |
| G2-Sim2 | 0.018 | 0.057 | | | |

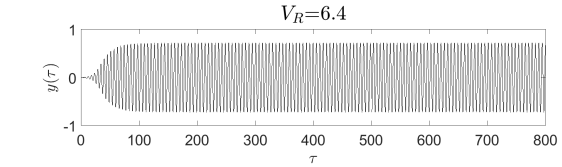


(a) Pure VIV.

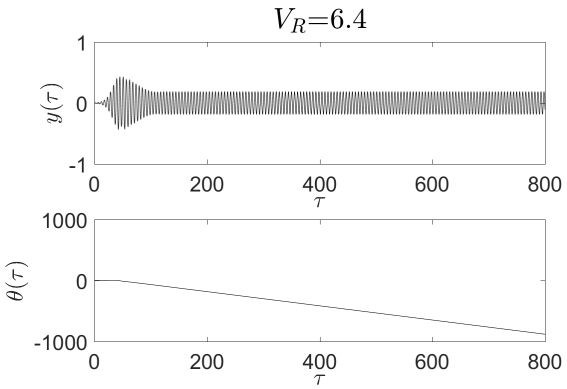


(b) G1-Sim5.

**FIGURE 6**: DISPLACEMENT TIME HISTORIES. $V_R = 6.4$.

in [8] for VIV and in [13] for galloping reveal amplitude modulations. This is an interesting aspect that will be investigated in a future paper. Notice, however, that the VIV response discussed in [8] is obtained from CFD at Reynolds number equal to 100, such that no information regarding the reduced velocity is provided in the mentioned paper.

## CONCLUSIONS

This paper presented a fundamental numerical study on VIV suppression using a rotative non-linear vibration absorber (NVA). The mathematical model was developed considering a rigid cylinder, free to oscillate in the cross-wise direction and coupled to the absorber. A wake-oscillator model represented the hydrodynamics loads. A parametric study enabled discussing the influence of each suppressor parameter on the response. Contrary to some previous works on the theme, which focused only on a few reduced velocities, the analyses herein presented covered the whole range of lock-in and certainly is a contribution of this paper.

Another contribution is the sensitivity study with respect to the influence of the NVA parameters on the cylinder characteristic oscillation amplitude. The simulations showed that the mass parameter $\hat{m}$ plays an important role in the VIV suppression. On the other hand, variations in the *radius* did not show significant influence on the maximum oscillation amplitude. The most important effect of the NVA radius is the narrowing of the lock-in range of reduced velocities.

Two quantitative criteria for the suppression were employed. The first criteria considers only the effects of the NVA on the peak of response, whereas the second one analyzes the whole range of reduced velocity. In addition to these criteria, an example of response of both the cylinder and the rotative NVA displacements was showed. Besides the marked reduction in the steady-state oscillation amplitude, it was observed that the NVA rotates with angular velocity practically constant, in agreement with previous works that employed the CFD approach. Such a character of the NVA response can be useful for energy harvesting.

This paper is the first of a series investigations on the use of NVA for the VIV phenomenon under development by the Offshore Mechanics Laboratory (LMO) group. Among other ongoing works, we highlight investigations focusing on the case in which the cylinder oscillates in both the in-line and the cross-wise directions, as well as some considerations regarding dissipated energy at the dashpot. As the rotative NVA also induces in-line responses, we expect that this solution is also efficient for suppressing two degrees-of-freedom VIV. Finally, we emphasize that, at least to the authors' knowledge, exper-

imental data on VIV suppression using NVAs is not found in the literature. In this way, the LMO group also plans a series of fundamental experiments aiming at numerical-experimental correlations.

## ACKNOWLEDGEMENTS

The first and the second authors are grateful to São Paulo Research Foundation (FAPESP) for their MsC and undergraduate scholarships, grants 2017/06016-7 and 2016/11080-3 respectively. FAPESP is also acknowledged for supporting a research project with focus on the use of NVAs on the mitigation of both VIV and parametric instability phenomena (grant 2016/20929-2). The third author is grateful to the Brazilian National Research Council (CNPq) for the grant 31595/2015-0.

## REFERENCES

[1] Blevins, R., 2001. *Flow-Induced Vibration*. Krieger.

[2] Païdoussis, M. P., Price, S. J., and de Langre, E., 2011. *Fluid-Structure Interactions - Cross-Flow-Induced Instabilities*. Cambridge University Press.

[3] Khalak, A., and Williamson, C. H. K., 1999. "Motions, forces and modes transitions in Vortex-Induced Vibration at low Reynolds number". *Journal of Fluids and Structures,* ***13***, pp. 813–851.

[4] Sarpkaya, T., 2004. "A critical review of the intrinsic nature of vortex-induced vibrations". *Journal of Fluids and Structures,* ***19***, pp. 389–447.

[5] Facchinetti, M. L., de Langre, E., and Biolley, F., 2004. "Coupling of structure and wake oscillators in vortex-induced vibrations". *Journal of Fluids and Structures,* ***19***, pp. 123–140.

[6] Ogink, R., and Metrikine, A., 2010. "A wake oscillator with frequency dependent coupling for the modeling of vortex-induced vibration". *Journal of Sound and Vibration,* ***329***(26), dec, pp. 5452–5473.

[7] Lee, Y. S., Vakakis, A. F., Bergman, L. A., McFarland, D. M., Kerschen, G., Nucera, F., Tsakirtzis, S., and Panagopoulos, P. N., 2008. "Passive non-linear targeted energy transfer and its applications to vibration absorption: a review". *Journal of Multi-body Dynamics,* ***222***(77-134).

[8] Blanchard, A. B., Gendelman, O. V., Bergman, L. A., and Vakakis, A. F., 2016. "Capture into slow-invariant-manifold in the fluid–structure dynamics of a sprung cylinder with a nonlinear rotator". *Journal of Fluids and Structures,* ***63***, may, pp. 155–173.

[9] Dai, H., Abdelkefi, A., and Wang, L., 2017. "Vortex-induced vibrations mitigation through a nonlinear energy sink". *Communications in Nonlinear Science and Numerical Simulation,* ***42***, jan, pp. 22–36.

[10] Tumkur, R. K. R., Pearlstein, A. J., Masud, A., Gendelman, O. V., Blanchard, A. B., Bergman, L. A., and Vakakis, A. F., 2017. "Effect of an internal nonlinear rotational dissipative element on vortex shedding and vortex-induced vibration of a sprung circular cylinder". *Journal of Fluid Mechanics,* ***828***, pp. 196–235.

[11] Franzini, G. R., Gonçalves, R. T., Meneghini, J. R., and Fujarra, A. L. C., 2012. "Comparison between force measurements of one and two degrees-of-freedom VIV on cylinder with small and large mass ratio". In Proceedings of the 10th FIV 2012 - International Conference on Flow-Induced Vibrations Conference (& Flow-Induced Noise).

[12] Freire, C. M., Korkischko, I., and Meneghini, J. R., 2011. "Defining a parameter of effectiveness for the suppression of vortex-induced vibration". In Proceedings of the ASME 2011 30th International Conference on Ocean, Offshore and Arctic Engineering - OMAE2011.

[13] Teixeira, B., Franzini, G. R., and Gosselin, F. P., 2018. "Passive suppression of transverse galloping using a non-linear energy sink". In Proceedings of the 9th International Symposium on Fluid-Structure Interactions, Flow-Sound Interactions, Flow-Induced Vibration & Noise (submitted).